
PHYSICS OF ELEMENTARY PARTICLES
AND ATOMIC NUCLEI. EXPERIMENT

Longitudinal Tomography of Ion Bunches in the JINR Superconducting Booster Synchrotron

V. M. Zhabitsky*

Joint Institute for Nuclear Research, Dubna, Moscow oblast, 141980 Russia

**e-mail: V.Zhabitsky@jinr.ru*

Received May 10, 2023; revised July 17, 2023; accepted July 17, 2023

Abstract—Methods for processing a digital signal proportional to the longitudinal intensity of ions in bunches during their acceleration in a synchrotron are discussed. Computer tomography is employed to reconstruct the longitudinal 2D ion distribution function in a bunch using data on its longitudinal profiles that depend on the bunch length and the synchrotron motion of particles. Presented are examples of tomographic reconstruction of the longitudinal distribution function of xenon ions in the JINR superconducting booster synchrotron prior to extraction (after acceleration) and on the injection plateau also with the activated electron cooling system.

DOI: 10.1134/S1547477123060419

INTRODUCTION

Computational tomography methods—mathematical algorithms for reconstructing the internal structure of an object from a set of projection data—are widely used in today’s research. Typically, projection data is obtained for a thin layer (slice of an object), the internal structure of which is described by a 2D distribution function. This class of objects includes bunches of charged particles circulating in a synchrotron. Indeed, the sensor of the pulsed current of circulating charged particles registers data along the length of the flying bunch, which correspond to the longitudinal intensity profile of the particles. The accelerated bunch is formed by particles undergoing stable synchrotron oscillations near the equilibrium state for a synchronous particle under the conditions of autophasing. Phase trajectories of accelerated particles with energies $E(t)$, different from the energy of the synchronous particle, $E_s(t_s)$, are closed curves. Their projections on the time axis set the longitudinal profile of the bunch $n(t - t_s)$ as a data set for intensities in bunch cross sections. Identification of deviations $E(t) - E_s(t_s)$ based on observed profiles $n(t - t_s)$ is the goal of reconstructing the 2D particle distribution function $f(E - E_s, t - t_s)$ in a bunch.

It was shown in [1] that the computational tomography for bunches of charged particles in a synchrotron makes it possible to reconstruct the longitudinal 2D distribution function of particles in a bunch. In studies [2, 3] the tomographic procedure for reconstructing the longitudinal phase portrait of ion bunches was applied at JINR Nuclotron [4]. New

publications on the use of the tomographic procedure algorithm are presented in [5, 6]. We describe below a set of processes for recording data on the bunch length and their subsequent mathematical processing to reconstruct the longitudinal 2D distribution function of ions in a bunch accelerated in the JINR superconducting booster synchrotron [7], where commissioning works are carried out at the NICA complex [8].

BASIC CONCEPTS

Observed analog signal $n(t)$, which is proportional to the longitudinal intensity of ion bunches during their acceleration in the synchrotron, is usually converted into a sequence of digital samples $n[i] \hat{=} n(t_i)$, which correspond to the moments of time $t_i = iT_{\text{clk}}$ with constant sampling period T_{clk} . The functional scheme for recording data on bunch intensities for tomographic reconstruction of the longitudinal phase portrait of an ion bunch in the superconducting booster synchrotron at JINR is shown in Fig. 1. This setup, which was successfully used at JINR Nuclotron, is described in detail in [2, 3].

During injection, five equidistant bunches are formed on the booster orbit (the RF harmonic number of the accelerating field frequency $h_{\text{rf}} = 5$). The intensity of the bunches is recorded by the fast current transformer FCT. The analog signal from the FCT is supplied to the first input of a two-channel digitizer, where it is converted into a sequence of digital samples $n[i]$ corresponding to the moments of time $t_i = iT_{\text{clk}}$ with constant sampling period $T_{\text{clk}} = 20$ ns and amplitude resolution

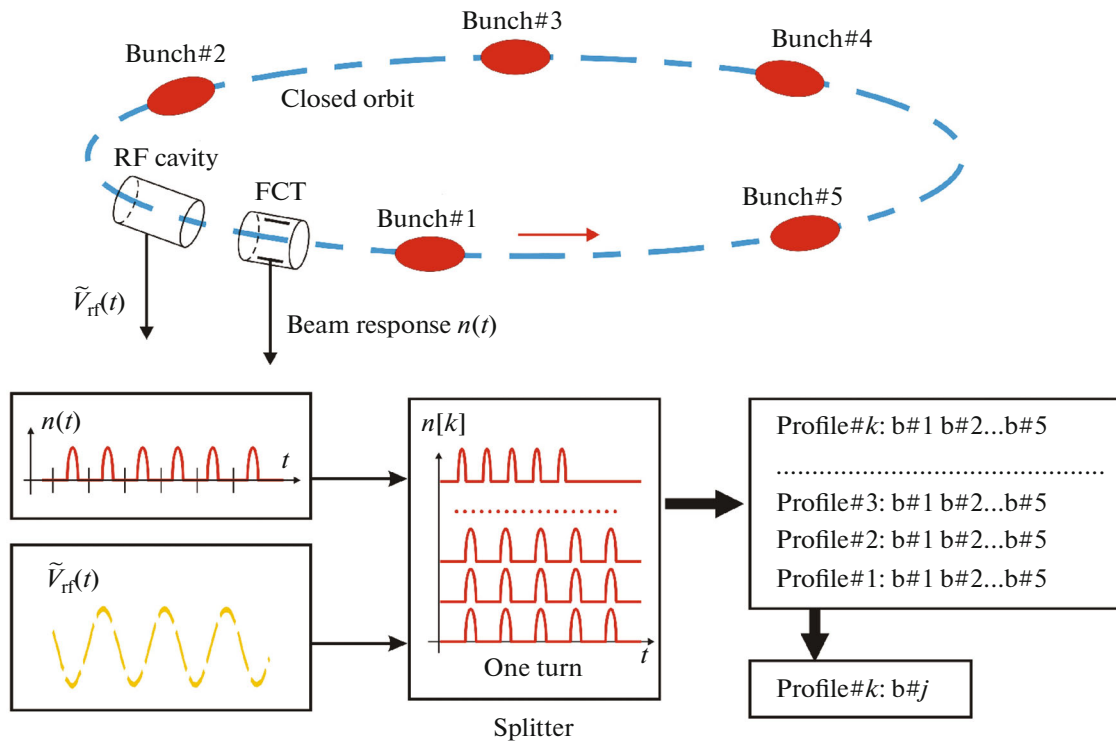


Fig. 1. Functional diagram of data logging.

$N_a = 14$ bit. Each such reading, being the result of measurements, corresponds to the observed signal, taking into account the measurement noise provided the Kotelnikov–Nyquist conditions are fulfilled [9].

The second input of the digitizer is supplied with a harmonic signal for accelerating stations $\tilde{V}_{rf}(t) = V_0 + V_{rf}(t) \cos(\omega_{rf}(t) + \varphi_0)$, whose cyclic frequency $\omega_{rf}(t)$ is set in accordance with the law of change of the magnetic field in dipoles $B(t)$ [10].

As a result, two digital signals are formed $n[i]$ and $\tilde{V}_{rf}[i]$, which are sent to a remote computer, where all the necessary signal processing and computer tomography procedures are carried out. First (see [11, 12]) these digital signals are jointly processed to transform a 1D data array $n[i]$ into a 3D array of data by samples i within the bunch with the number j on the revolution k . The base level of the FCT signal is shifted in such a way that, within the bunch, the measured data correspond to a positively defined finite function. Then a 3D data array is converted into projection data $f[i, j, k]$ for h_{rf} bunches needed for a tomographic procedure starting at time t_{init} . And, finally, data for intensity profiles $f_j[i, j, k]$ are generated for a specific bunch j for which the computed tomography procedure is performed.

The described procedure for proceedings from a digital signal $n[i]$ for the pulse intensity of circulating

bunches to the functions $f_j[i, j, k]$, which are a characteristic of the differential distribution law of particles in bunch j on revolution k , makes it possible to identify the projection data needed for the computer tomography algorithm. The correctness of this procedure is controlled visually by constructing a 3D plot for the obtained profiles. The delay value of the digital signal $\tilde{V}_{rf}[i]$ is selected in such a way that all profiles for $n[i]$ consistently follow one after the other. This procedure is additionally checked using a plot for the number of particles in the bunch [11], which should correspond to a constant (or decreasing in the case particles are lost) function.

To reconstruct the phase portrait from the data for the longitudinal profiles of a particular bunch, study [1] used the iterative procedure ART [13]. It can be applied at the time t_{init} for ions circulating along an orbit with a perimeter $C_0 = 2\pi R_0$ with rest mass m and charge q if the magnetic field induction in dipoles B and the rate of its change \dot{B} , the accelerating field V_{rf} , the rate of its change \dot{V}_{rf} , the RF harmonic number of the accelerating field h_{rf} , radius of curvature of the trajectory in dipoles ρ , and the relativistic factor for the critical energy γ_{tr} are known. The period of synchrotron oscillations T_s expressed in terms of the particle circulation period T_{rev} increases with an increase in the oscillation amplitude [10]. The more compact the

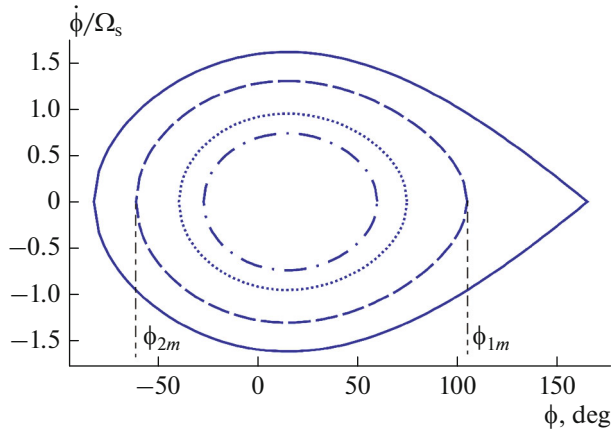


Fig. 2. Scheme of the phase selection procedure.

bunch, the more accurate procedure [13] applied in [1]. Therefore, the result of the phase portrait reconstruction should correspond to a convergent iterative procedure, for which a criterion is specified in [13]: the estimate D^q characterizing the discrepancy between the measured and calculated projections as a function of the number of iterations.

A feature of the observed signal $n(t)$ when xenon ions ${}_{124}\text{Xe}^{28+}$ were accelerated in the booster during commissioning operations was its low intensity against the background of measuring noise. To distinguish the differential distribution function of particles in a bunch against the noise background, we used the phase selection procedure [2, 3]. Accelerating voltage V_{rf} corresponds to the height of the separatrix for phase trajectories (see Fig. 2), which is proportional to the maximum allowable deviation of the particle energy ΔE_{max} from equilibrium [10]. The longitudinal distribution function of particles in a bunch usually corresponds to a Gaussian distribution. Consequently, the number of particles in the space of phase trajec-

ries outside the trajectory with height ΔE near the trajectory for ΔE_{max} is not large. Therefore, it is possible to limit the array of processed data to the phase trajectory $\Delta E < \Delta E_{\text{max}}$. As a result of applying this procedure, a positive-definite finite function is formed, which has non-zero values only inside a given phase trajectory $\phi \in [\phi_{2m}, \phi_{1m}]$ (see Fig. 2).

PHASE PORTRAIT OF THE BUNCH IN THE PROCESS OF BEING EXTRACTED FROM THE BOOSTER

To fulfill the conditions for the transfer of charged particles from the booster to Nuclotron on the intermediate plateau of the magnetic field cycle in the booster, five bunches are ungrouped and the expanded beam is then grouped into a single bunch [7]. Plots of $n[i]$ and $\tilde{V}_{\text{rf}}[i]$ on the output plateau are shown in Fig. 3a (a fragment is reproduced in the range $t \in [0.580007, 0.580015]$ s for $k = 6$ revolutions). Fitting an array of measured data at $k = 7767$ revolutions (see Fig. 3b, $t \in [0.586, 0.596]$ s) for the period of revolution of a single bunch on the output plateau yields a statistical estimate of the value $T_{\text{rev}} = T_{\text{rf}} = 1.23066 \mu\text{s}$ (systematic error ± 20 ns in accordance with T_{clk}). The magnetic field induction in dipoles on the output plateau was $B = 0.683903$ T. For the design length of the orbit in the booster $C_0 = 210.96$ m according to the data for T_{rev} the radius of curvature of the ion trajectory in the dipole was calculated to be $\rho = 14.0 \times 1.0051$ m. The resulting value of ρ is somewhat more than the design value $\rho = 14.0$ m.

Figure 4a displays a 3D plot of the evolution of the longitudinal profiles of the FCT signal in the time interval $t \in [586, 587]$ ms. A projection of 3D plot onto the $(k \times \tau)$ plane is shown in Fig. 4b. The 2D plot makes it possible to check the correctness of the procedures applied for synchronizing signals from the

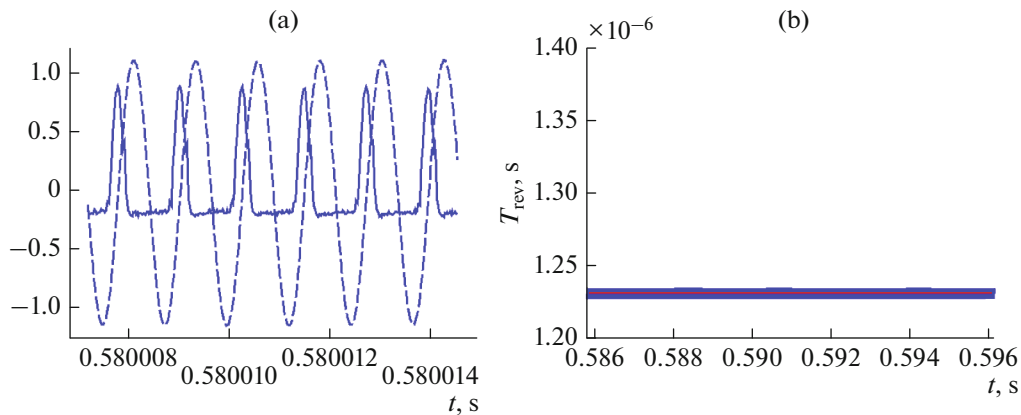


Fig. 3. (a) $n[i]$ (solid line) and $\tilde{V}_{\text{rf}}[i]$ (dashed line); (b) $T_{\text{rev}}[k]$, $k \in [0, 7767]$.

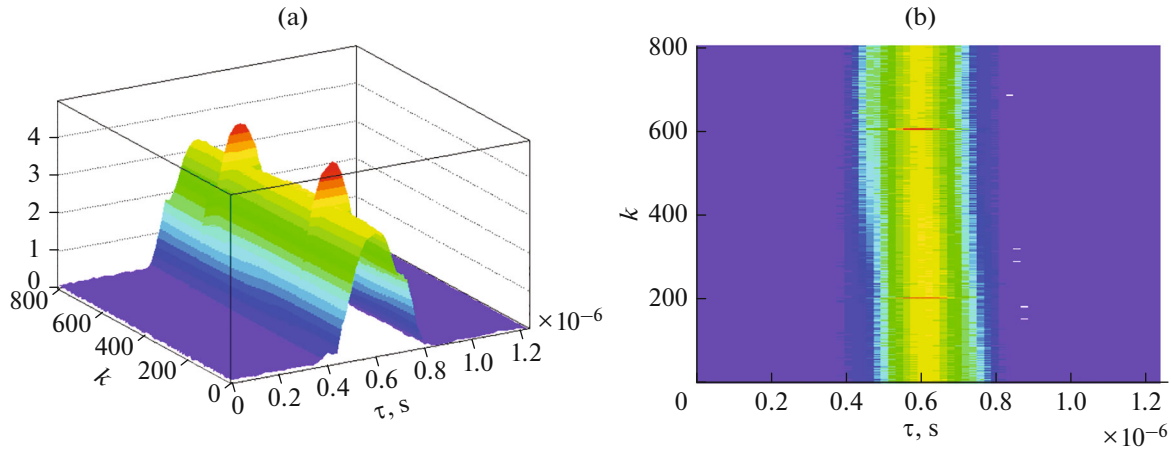


Fig. 4. (a) 3D plot and (b) 2D plot of an intensity profile.

FCT and from the accelerating section: on the magnetic field plateau $\dot{B} = 0$ and synchronous phase $\varphi_s = 0$. Consequently, the bunch center should be located at $\tau = T_{\text{rf}}/2$. A plot displayed in Fig. 4b confirms that the synchronization conditions are fulfilled. A 3D plot in Fig. 4a indicates oscillations in the bunch shape, which makes it possible to estimate the value $T_s/T_{\text{rev}} \approx 1600$ and hence the effective accelerating field V_{rf} .

Thus, all the quantities necessary for the application of the tomographic procedure were determined by analyzing the data on the evolution of longitudinal profiles for the bunch intensities, taking into account the design specifications of the booster.

Figure 5c shows the phase portrait of the bunch under study. This result was obtained taking into account the application of the phase selection procedure at $\Delta E = 0.98\Delta E_{\text{max}}$. At $\Delta E = \Delta E_{\text{max}}$ the specific weight of the peripheral components of the data array for the longitudinal profiles is significant due to the measurement noise. As a result, the central region for small amplitudes of synchrotron oscillations is poorly reconstructed. Thus, the use of the phase selection procedure (limitation of the reconstructed longitudinal energy spread in the presence of a noise component in the processed digital signal) makes it possible to provide the necessary reconstruction of the longitudinal phase portrait of the ion bunch for small amplitudes of synchrotron oscillations.

PHASE PORTRAIT OF A BUNCH ON THE INJECTION PLATEAU

The ion beam is injected from the linear accelerator on the plateau of magnetic field injection in the booster with the RF system turned off. As a result, the injected bunch is ungrouped. After about 135 ms, an accelerating voltage is applied to the accelerating sys-

tem, and 5 bunches are formed (the RF harmonic number of the accelerating field $h_{\text{rf}} = 5$). Figure 6 shows 2D plots of the evolution of the longitudinal profiles of formed bunches ($t \in [120, 200]$ ms) with the electron cooling system turned off and on [14]. The tomographic procedure is applied to the last 10 ms of the digital data array, since when the accelerating RF system is turned on, the bunch formation is accompanied by some beam losses.

Figure 7 shows 2D plots of the evolution of the longitudinal profiles of formed bunches prepared for the application of the tomographic procedure ($t \in [190, 200]$ ms). To do this, with the electron cooling system turned off, for detuning from noise, the phase selection procedure was used to select phase trajectories lying inside the trajectory $\Delta E = 0.92\Delta E_{\text{max}}$ (see Fig. 7a). In addition to the phase selection procedure, a rebinning procedure was applied in accordance with the algorithm presented in [1]. This procedure is reduced to averaging data for longitudinal profiles over several revolutions k_{av} , which somewhat improves the phase portrait resolution ($k_{\text{av}} = 2$ for the profiles displayed in Fig. 7a).

With the electron cooling system turned on, the bunch is more compact. Therefore, it is sufficient to use the phase selection procedure to select phase trajectories that are located inside the trajectory $\Delta E = 0.98\Delta E_{\text{max}}$ (see Fig. 7b).

It should be noted that the driving frequency supplied to the accelerating station and the rate of switching on the accelerating voltage were not chosen very carefully. Therefore, particles were grouped into bunches with significant coherent synchrotron oscillations (see Fig. 6). However, the graphic dependences displayed clearly demonstrate the operability of the electron cooling system. The measurements were carried out on January 25, 2023, at 16:07:07 (electron

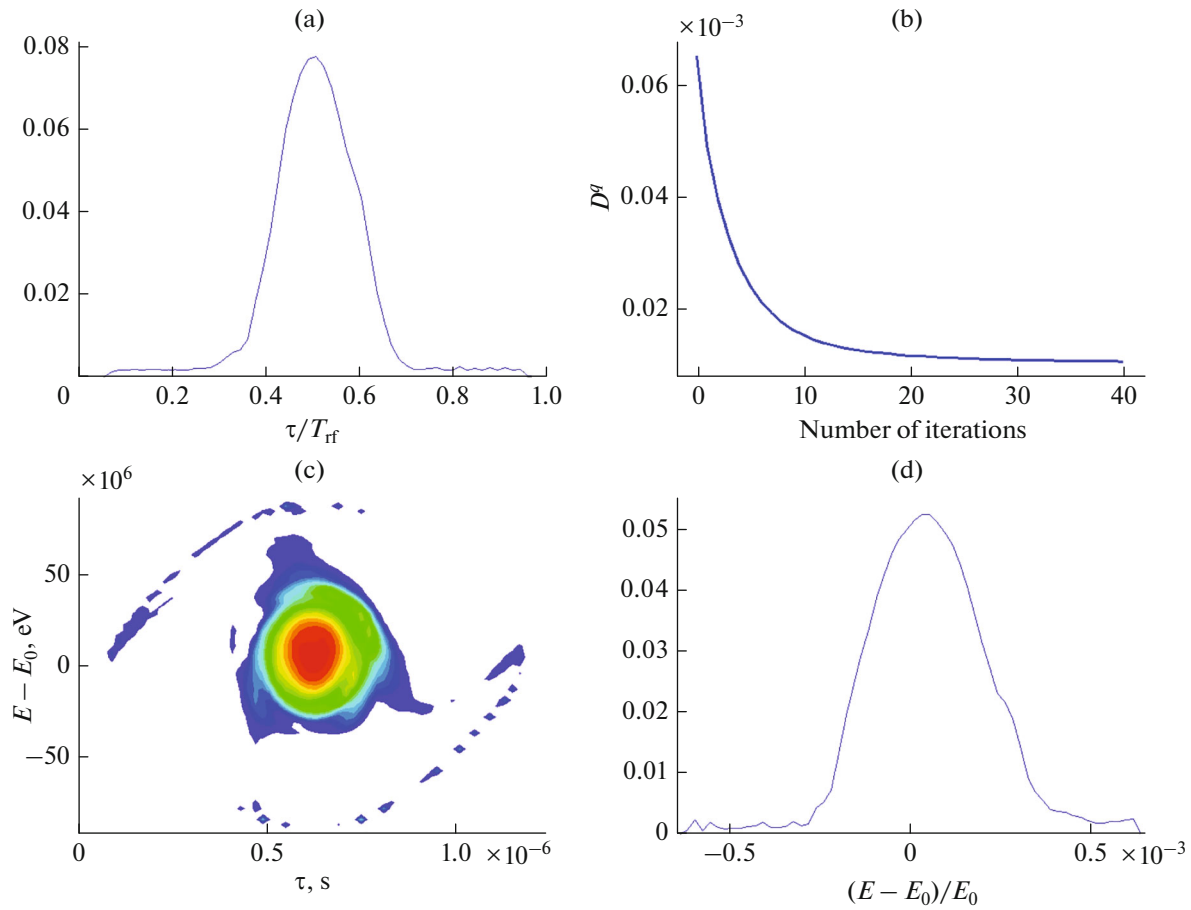


Fig. 5. (c) phase portrait and its corresponding distribution functions (a) in time and (d) in energy; (b) plot of D^q vs the number of iterations.

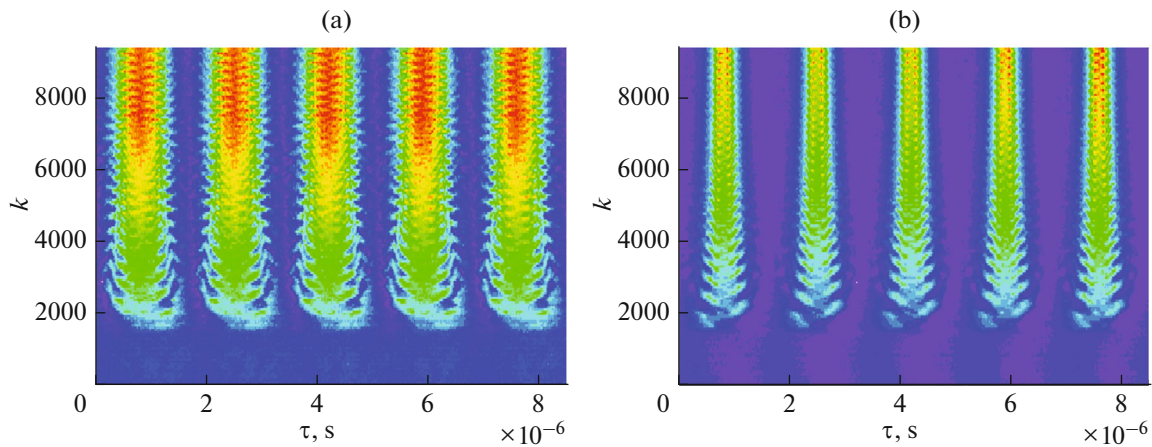


Fig. 6. Electron cooling system is (a) off and (b) on.

cooling system turned off) and at 16:10:19 (electron cooling system turned on). Graphic dependences presented in Fig. 7 confirm that the conditions for synchrotron motion with respect to the parameter T_s/T_{rev} are identical.

The results of reconstructing the phase portraits of the ion bunch are shown in Figs. 8. With the electron cooling system being turned on, the bunch is compact. However, when the cooling system is turned off, the particles are distributed along almost the entire length

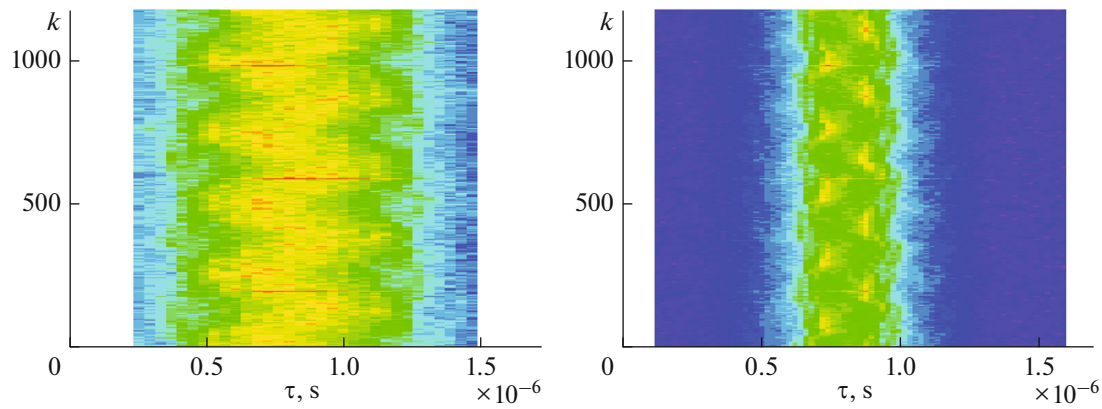


Fig. 7. Profiles for tomography: the electron cooling system is (a) off and (b) on.

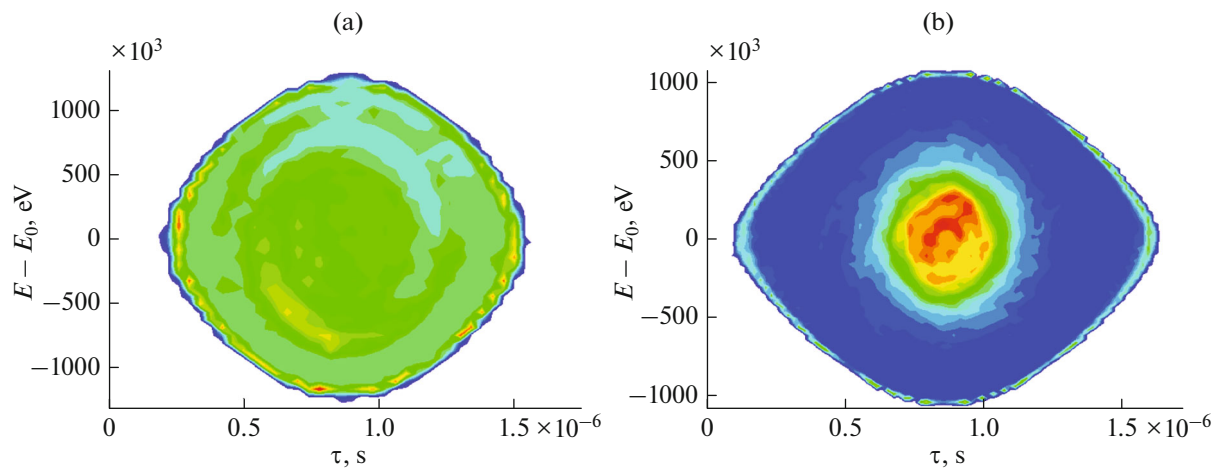


Fig. 8. Phase portrait of a bunch: the electron cooling system is (a) off and (b) on.

of the bunch, which is consistent with the data on the longitudinal profiles shown in Fig. 7a. The root-mean-square spread in the energies of the formed bunch is approximately $\sigma_E = 4.1 \times 10^{-6}$ when the electron cooling system is turned off, which is significantly smaller than the same estimate for the expanded beam obtained in [15]. This result is in agreement with the observed losses of charged particles during the formation of five bunches on the injection plateau.

CONCLUSIONS

The method of tomographic reconstruction of the longitudinal phase portrait of an ion bunch in the JINR superconducting booster synchrotron has been successfully applied.

It has been established that the use of the phase selection procedure (limitation of the reconstructed longitudinal energy spread in the presence of a noise component in the processed digital signal) makes it possible to provide the necessary reconstruction of the

longitudinal phase portrait of an ion bunch for small amplitudes of synchrotron oscillations.

Examples are given of reconstructed phase portraits of a xenon ion bunch after acceleration in the booster and after injection, also with the electron cooling system turned on.

ACKNOWLEDGMENTS

The author is grateful to all participants in the commissioning work at the JINR booster for the opportunity to conduct tomographic studies.

CONFLICT OF INTEREST

The authors declare that they have no conflicts of interest.

OPEN ACCESS

This article is licensed under a Creative Commons Attribution 4.0 International License, which permits use, shar-

ing, adaptation, distribution and reproduction in any medium or format, as long as you give appropriate credit to the original author(s) and the source, provide a link to the Creative Commons license, and indicate if changes were made. The images or other third party material in this article are included in the article's Creative Commons license, unless indicated otherwise in a credit line to the material. If material is not included in the article's Creative Commons license and your intended use is not permitted by statutory regulation or exceeds the permitted use, you will need to obtain permission directly from the copyright holder. To view a copy of this license, visit <http://creativecommons.org/licenses/by/4.0/>.

REFERENCES

1. S. Hancock, P. Knaus, and M. Lindroos, "Tomographic measurements of longitudinal phase space density," in *Proceedings of the Sixth European Particle Accelerator Conference, Stockholm, Sweden, 1998* (Inst. Phys., 1998), pp. 1520–1522; CERN-PS-98-030-RF (CERN, Geneva, 1998). URL: <https://cds.cern.ch/record/363824>.
2. V. M. Zhabitsky, "Computerized tomography of ion bunches at the Nuclotron," *Phys. Part. Nucl. Lett.* **15**, 767–773 (2018). URL: http://www1.jinr.ru/Pepan_letters/panl_2018_7/14_Zhabitsky.pdf.
3. V. M. Zhabitsky, "Tomographic reconstruction of the longitudinal distribution function of ions in bunches during acceleration at the Nuclotron," in *Proceedings of the 26th Russian Particle Accelerators Conference RuPAC-2018, Protvino, Russia, 2018*, pp. 128–131. URL: <https://accelconf.web.cern.ch/rupac2018/papers/thzmmh01.pdf>.
4. A. Sidorin, N. Agapov, A. Alfeev, et al., "Status of the Nuclotron," in *Proceedings of the 26th Russian Particle Accelerators Conference RuPAC-2018, Protvino, Russia, 2018*, pp. 49–51. URL: <https://accelconf.web.cern.ch/rupac2018/papers/tuzmh04.pdf>.
5. C. H. Grindheim and S. Albright, "Longitudinal phase space tomography version 3," Tech. Rep. CERN-ACC-NOTE-2021-0004 (CERN, Geneva, 2021). URL: <https://cds.cern.ch/record/2750116>.
6. T. Argyropoulos et al., "RF power at injection and longitudinal tomography," Tech. Rep. LHC Chamonix Workshop 2023, 2023 (CERN, Geneva, 2023). URL: <https://indico.cern.ch/event/1224987/contributions/5153690/>.
7. A. Butenko, H. Khodzhbagiyani, S. Kostromin, et al., "The NICA complex injection facility," in *Proceedings of 27th Russian Particle Accelerators Conference RuPAC-2021, Alushta, Russia, 2021* (JACoW Publishing, 2021), pp. 7–11. URL: <https://accelconf.web.cern.ch/rupac2021/papers/moy01.pdf>.
8. E. Syresin, N. Agapov, A. Alfeev, et al., "NICA ion collider at JINR," in *Proceedings of 27th Russian Particle Accelerators Conference RuPAC-2021, Alushta, Russia, 2021* (JACoW Publishing, 2021), pp. 12–16. URL: <https://doi.org/10.18429/JACoW-RuPAC2021-MOY02>
9. I. S. Gonorovsky, *Radio Circuits and Signals* (Sovetskoye Radio, Moscow, 1977) [in Russian].
10. G. Bruk, *Cyclic Charged Particle Accelerators* (Atomizdat, Moscow, 1970) [in Russian].
11. V. M. Zhabitsky, "Digital methods for diagnostics of longitudinal bunch parameters in synchrotrons," *Phys. Part. Nucl. Lett.* **13**, 127–131 (2016). URL: http://www1.jinr.ru/Pepan_letters/panl_2016_1/16_zhabit.pdf.
12. V. M. Zhabitsky, "Methods of computer processing of experimental data on the intensity of bunches in synchrotrons," *Phys. Part. Nucl. Lett.* **13**, 829–832 (2016). URL: http://www1.jinr.ru/Pepan_letters/panl_2016_7/15_zhabitsky.pdf.
13. R. A. Gordon, "Tutorial on ART," *IEEE Trans. Nucl. Sci.* **NS-21**, 78–93 (1974). URL: https://www.researchgate.net/publication/260355748_A_Tutorial_on_ART_Algebraic_Reconstruction_Techniques.
14. S. Semenov, A. Kobets, S. Kolesnikov, et al., "Commissioning of electron cooling system of NICA booster," in *Proceedings of the 26th Russian Particle Accelerators Conference RuPAC-2018, Protvino, Russia, 2018* (JACoW Publ., Geneva, Switzerland, 2018) URL: <https://accelconf.web.cern.ch/rupac2018/papers/tup-sa22.pdf>, ISBN: 978-3-95450-197-7.
15. V. M. Zhabitsky, "Methods for monitoring the longitudinal momentum spread of ions within a bunch during an injection into a synchrotron," *Phys. Part. Nucl. Lett.* **19**, 803–807 (2022). URL: http://www1.jinr.ru/Pepan_letters/panl_2022_6/15_Zhabitsky.pdf.